CHIN. PHYS. LETT. Vol. 37, No. 2 (2020) 025201

Phase Effects of Long-Wavelength Rayleigh–Taylor Instability on the Thin Shell *

Zhi-Yuan Li(李志远)[1], Li-Feng Wang(王立锋)[1,2], Jun-Feng Wu(吴俊峰)[1], Wen-Hua Ye(叶文华)[1,2**]

[1]*Institute of Applied Physics and Computational Mathematics, Beijing 100094*

[2]*Center for Applied Physics and Technology, HEDPS, and College of Engineering, Peking University, Beijing 100871*

(Received 27 September 2019)

Taking the long-wavelength Rayleigh–Taylor instability (RTI) on the thin shell of inertial confinement fusion as the research object, a linear analytical model is presented to study the phase effects that are caused by the phase difference of single-mode perturbations on the two interfaces. Its accuracy is tested by numerical simulations. By analyzing the characteristic of this model, it is found that the phase difference does not change the basic RTI structure (only one spike and one bubble in a period). However, the symmetry of the spike and bubble is destroyed, which has non-expected influences on the convergent motion of ICF targets. Meanwhile, the phenomenon that the distance between spikes and bubbles along the vertical direction of acceleration differs by π is demonstrated. It is also shown that when the phase difference is large, the temporal evolution of the RTI is more serious and the thin target is easier to tend to break.

PACS: 52.57.Fg, 47.20.Ma, 52.35.Py DOI: 10.1088/0256-307X/37/2/025201

The Rayleigh–Taylor instability[1,2] will happen when a heavy fluid is accelerated by a lighter fluid, which happens if some perturbations are on the interface between two fluids. This is a common phenomenon in the implosion experiments of inertial confinement fusion (ICF).[3] Researchers have shown that the existence of the RTI is one of the most important reasons for the ignition failure of NIF.[4] In particular, when the shell is relatively thin, perturbations on one interface feed through to another interface can be crucial.[4,5]

The RTI on the thin shell contains multi-interfaces. The classic RTI models,[1,2] which only include a single material interface, are not enough for depicting this kind of perturbation growth. Researchers have taken some efforts to understanding its mechanism. The first series of studies were made by Mikaelian. The author used the mode analysis method to describe the temporal evolution of the RTI in the linear growth regime at the interfaces of any number of stratified fluids forming an arbitrary density profile.[6] The author has extended the model in plane geometry to that in cylindrical geometry.[7] Following Mikaelian's works, the weakly nonlinear (WN) growth regime of the RTI was taken into consideration by Wang *et al.*[8] They presented an analytical WN model of the RTI with a finite-thickness fluid layer and pointed that the weakly nonlinear effect and interface thickness effect are important for understanding the flow phenomenons of ICF. Recently, the linear growth of Rayleigh–Taylor instability of two finite-thickness fluid layers was studied by Guo *et al.*[9] using an analytical model. Besides the analytical works, some experiments demonstrated that the perturbation coupling between interfaces has pronounced influences on the development of the RTI.[10,11]

However, there are almost no studies focusing on the situations with the phase effect. Because the perturbations on the surface of the pellet are random, the RTI with phase difference is common in the process of ICF implosion. In this Letter, the phase effects of the RTI on a thin shell are studied by a linear analytical model. First, the model is presented, and its reliability and application scope are evaluated by a well-tested Euler code. Second, in terms of the thin shell target in the acceleration regime of ICF, the analytical model is applied to study the phase effects on the evolution of the RTI. For this study, the thickness of the target is 20 μm. The wavelength of perturbation, which is larger than 100 μm, is focused. Consequently, the interface coupling effects are obvious. If not otherwise specified, the RTI in the following is the one on the thin target with two interfaces.

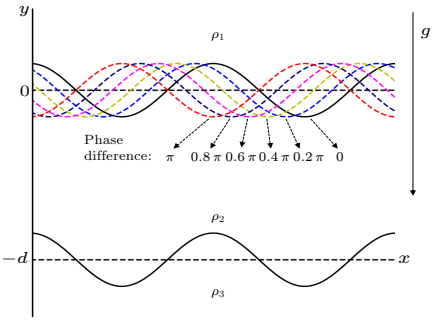

Fig. 1. Schematic drawing about the initial condition of the RTI with double interfaces.

For the thin shell target in the acceleration regime of ICF, the density ratios at the two interfaces are close to 1 and the acceleration is huge.[8] As an approximation, we use the model shown in Fig. 1 to represent the target. Along the direction of acceleration, a finite-thickness fluid layer with density $\rho_2 = 1\,\mathrm{g/cm^3}$ is located between two semi-infinite vacuum layers.

*Supported by the National Natural Science Foundation of China under Grant Nos. 11575033, 11675026 and 11975053, and the CAEP Foundation under Grant No. CX2019033.

**Corresponding author. Email: ye_wenhua@iapcm.ac.cn

© 2020 Chinese Physical Society and IOP Publishing Ltd

The thickness of the shell is d. Single-mode cosinusoidal perturbations defined as $\eta(0) = \eta_0 \cos(kx + \alpha)$ are set on the two interfaces. Here η_0 is the amplitude of the initial perturbation; k is the wavenumber; α is the phase. The α at the lower interface is a constant of zero. The phase difference is changed by adjusting α on the upper interface.

As the long-wavelength RTI is focused, the viscosity effect and the stabilization effect of the ablative Rayleigh–Taylor instability are not obvious.[12] Meanwhile, the compressibility can be ignored when the shock wave comes through. The potential flow model can be used to describe the linear evolution of the RTI in the acceleration regime of ICF. For the situations $\alpha = 0$ and $\alpha = \pi$, the existing analytical model[8] can depict their linear evolutions. If there is no perturbation on the lower interface, the linear evolution of the two interfaces can be expressed as

$$\eta^u_{1,0}(t) = \Xi \left[a\cos(\gamma t) - e^{-2kd} a \cosh(\gamma t)\right] \cos(kx), \quad (1)$$

$$\eta^l_{1,0}(t) = \Xi e^{-kd} a \left[\cos(\gamma t) - \cosh(\gamma t)\right] \cos(kx), \quad (2)$$

where $\Xi = 1/(1 - e^{-2kd})$; $\gamma = \sqrt{kg}$ is the linear growth rate with g being the acceleration; a is η_0 on the upper interface. In addition, if there is no perturbation on the upper interface, then the linear evolution of the two interfaces can be expressed as

$$\eta^u_{0,1}(t) = \Xi[-e^{-kd} b \cos(\gamma t) + e^{-kd} b \cosh(\gamma t)]\cos(kx+\alpha), \quad (3)$$

$$\eta^l_{0,1}(t) = \Xi[-e^{-2kd} b \cos(\gamma t) + b \cosh(\gamma t)]\cos(kx+\alpha), \quad (4)$$

where b is η_0 on the lower interface. It is shown that the perturbation on one interface can transport to another one by a damping factor which is related to e^{-kd}. Based on the principle of linear superposition, if there are perturbations simultaneously on the two interfaces, then the upper interface evolution will be the additive effects of Eqs. (1) and (3), and the lower interface evolution would be the additive effects of Eqs. (2) and (4). In this way, the linear RTI evolution of two interfaces can be defined as

$$\begin{aligned} \eta^u(t) &= \eta^u_{1,0}(t) + \eta^u_{0,1}(t), \\ \eta^l(t) &= \eta^l_{1,0}(t) + \eta^l_{0,1}(t). \end{aligned} \quad (5)$$

Under the conditions $\alpha = 0$ and $\alpha = \pi$, Eq. (5) is the same as the linear model given by Wang *et al.*[8] Besides these two conditions, the one with an arbitrary α can also be depicted by Eq. (5). In this way, the effects of phase difference could be studied if Eq. (5) is reliable. To test its reliability along with its application scope, numerical simulations have been performed. The simulations are carried out by a second-order Euler Godunov hydrodynamic simulation code. The computational domain is $L \times 10L$, where L is equal to the wavelength λ. Approximately, the two semi-infinite vacuum layers are filled with the gas in density $0.01\,\mathrm{g/cm^3}$, which means that $\rho_1 = \rho_3 = 0.01\,\mathrm{g/cm^3}$. The acceleration g is $1000\,\mathrm{cm/\mu s^2}$. As shown in Fig. 1, the boundaries at the ends of the y direction are walls. At the ends of x direction, the periodic boundary condition is used. There are 256 uniform grids in the x direction and 2000 grids in the y direction. Most of the grids are located in the evolution region of the perturbation. To evaluate the numerical code, the benchmarks for the two interfaces in phase and in anti-phase are made. To make sure that the code is accurate enough to test the linear model, the analytical results are calculated by the WN model.[8] Figure 2 presents the temporal evolutions of the fundamental mode given by the analytical model and the numerical simulation. Here the wavelength is $100\pi\,\mu\mathrm{m}$ ($kd = 0.4$). The initial perturbation amplitude on the two interfaces are 0.01λ. The fundamental mode of numerical simulation is calculated by the Fourier transform of the areal density. Figure 2(a) depicts the temporal evolution of the lower interface. Figure 2(b) depicts the temporal evolution of the upper interface. The contours of condition a and condition b are also presented in the figure. It is shown that the fundamental modes given by our numerical simulation and the analytical model are almost consistent prior to the WN regime. Meanwhile, the interface shape obtained by the numerical simulation is close to the analytical one. Therefore, the Euler simulation is accurate enough to evaluate Eq. (5).

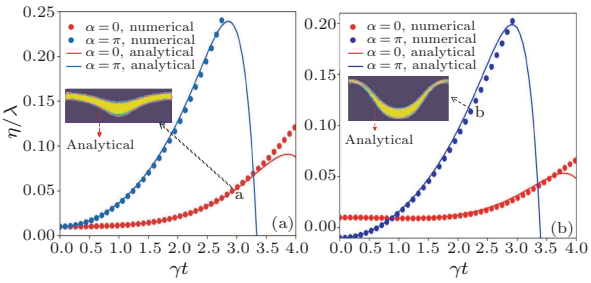

Fig. 2. Comparisons between the numerical results and the analytical results: (a) lower interface, (b) upper interface.

In terms of the evaluation of Eq. (5), the impacts of α, kd, a and b are taken into consideration in this study. Seven different combinations of initial conditions listed in Table 1 are tested.

Table 1. Initial conditions used to test the linear analytical model.

	α/π	kd	$a\lambda$	$b\lambda$		α/π	kd	$a\lambda$	$b\lambda$
a	0.2	0.4	0.01	0.01	e	0.4	0.8	0.01	0.01
b	0.4	0.4	0.01	0.01	f	0.4	0.4	0.005	0.01
c	0.6	0.4	0.01	0.01	g	0.4	0.4	0.01	0.005
d	0.4	0.6	0.01	0.01					

Equation (5) can be divided into a sine term and a cosine term. Their coefficients on the lower interface are represented by $\eta^l_{\sin}$ and $\eta^l_{\cos}$. In the same way, their coefficients on the upper interface are represented by $\eta^u_{\sin}$ and $\eta^u_{\cos}$. Under the conditions of a–g shown in Table 1, the temporal evolutions of these four coefficients are depicted in Figs. 3(a)–3(d), respectively.

The numerical setup is the same as the one of

Fig. 2. The lines and points in Fig. 3 are the results of our numerical simulation and the analytical model. Under the same initial condition, the colors of the line and points are the same. It is shown that, in the initial stage of the RTI evolution, the analytical model can present accurate results. Taking the initial condition d (black points) as an example, the analytical model can present the accurate $\eta^l_{\sin}$, $\eta^l_{\cos}$, $\eta^u_{\sin}$ and $\eta^u_{\cos}$ before $\gamma t \approx 2.5$. At this time, $\eta^l_{\sin} \approx -0.05\lambda$, $\eta^l_{\cos} \approx 0.07\lambda$, $\eta^u_{\sin} \approx -0.04\lambda$ and $\eta^u_{\cos} \approx 0.04\lambda$. After that, the RTI evolution will reach the WN regime, which is out of the application of the linear analytical model. The comparisons of the interfaces' shape given by the numerical simulation and the analytical model are also depicted in Fig. 3. Four conditions before the WN regime are presented. The dotted red lines in the contours are the results of Eq. (5). It is shown that the analytical model can present correct upper and lower interface shapes. Based on the results shown in Fig. 3, an overall evaluation about Eq. (5) is given in the following. Generally, Eq. (5) is applicative before the amplitude of the sine term and cosine term reach 0.05λ. Under some conditions, its application scope can be extended to 0.1λ. This is meaningful because there is long enough time to study the RTI evolution with interface phase difference. In the following, the linear analytical model will be applied to study the impacts of the phase difference on the RTI evolution of the thin shell target.

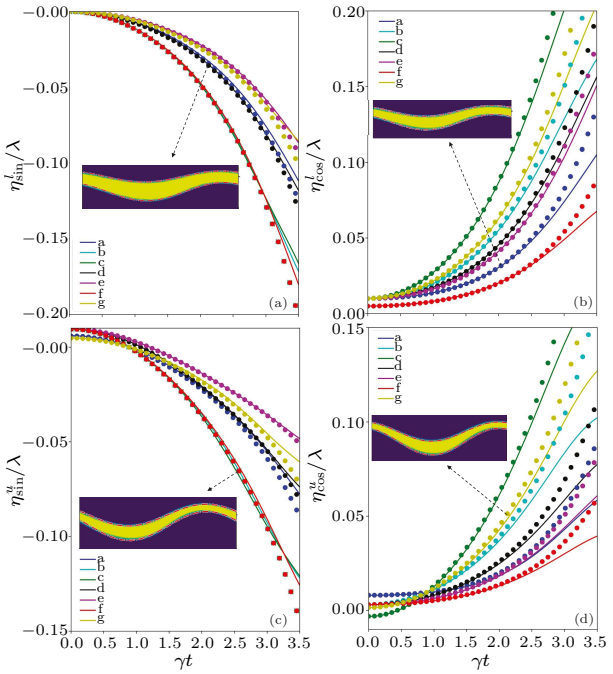

Fig. 3. Comparisons between the numerical results (lines) and the analytical results (points) on the fundamental mode growth along with the comparisons of the interface shape change.

First, the problems how the phase difference impacts on the interface shape and on the motion of target are studied. As shown in Fig. 3, there are only one spike and one bubble structure in a period under the initial conditions of a–g. In terms of other conditions, it is wonderful if the same rule is satisfied. To prove this problem, the evolution function of the interface (Eq. (5)) is written as

$$\eta(\theta) = c_1 \cos\theta + c_2 \sin\theta, \quad 0 \le \theta < 2\pi, \tag{6}$$

where θ is the kx in Eq. (5); c_1 and c_2 are the coefficients related to kd, a, b, γt and α. As kd, a, b, γt and α are arbitrary, c_1 and c_2 can be any real numbers. Here $0 \le \theta < 2\pi$ is focused as the period of Eq. (6) is 2π. When c_1 or c_2 is zero, $\eta(\theta)$ is dominated by $\cos(\theta)$ or $\sin(\theta)$. In this way, there is only one spike and bubble structure in one period. When c_1 and c_2 are not equal to zero, the number of spike and bubble can be judged by the characteristic of Eq. (6). Taking the partial derivative with respect to θ, we can obtain

$$\eta' = c_1 \sin\theta - c_2 \cos\theta. \tag{7}$$

If $\cos(\theta) = 0$ when $\eta' = 0$, $\sin(\theta)$ would be zero as c_1 and c_2 are not equal to zero. This is impossible as there is no θ making $\cos(\theta)$ and $\sin(\theta)$ equal to zero simultaneously. In this way, when $\eta' = 0$, the extreme values of Eq. (6) satisfy the equation $\tan\theta = \frac{c_2}{c_1}$. Here $\tan\theta$ is a monotone periodic function, and its period is π. Therefore, there are two extreme values when $0 \le \theta < 2\pi$, and these two extreme values differ by π. To judge that the extreme values are maximal or minimal (the position of spike or the position of bubble), Eq. (7) is transformed to

$$\eta' = \cos\theta(c_1 \tan\theta - c_2). \tag{8}$$

Conveniently, the two extreme values are represented by θ_1 and $\theta_1 + \pi$. The adjacent points of the two extreme values are $\theta_1 + \Delta\theta$ and $\theta_1 + \pi + \Delta\theta$. Therefore, near the two extreme values, η's are $\cos(\theta_1 + \Delta\theta)(c_1 \tan(\theta_1 + \Delta\theta) - c_2)$ and $-\cos(\theta_1 + \Delta\theta)(c_1 \tan(\theta_1 + \Delta\theta) - c_2)$, respectively. In this way, one of θ_1 and $\theta_1 + \pi$ is a maximal value, and the other is a minimal value. With this analysis, one can see that there must be only one spike and one bubble structure under a period under conditions with an arbitrary phase difference. The distance between the spike and bubble along the vertical direction of acceleration differs by π in the linear RTI regime.

Although one spike and one bubble in a period can be maintained when there is a phase difference in the thin target, the axial symmetry can be destroyed due to the existence of the sine term in Eq. (6). This can change the spatial position along the perpendicular direction of the acceleration, which makes the spike and bubble distort. Consequently, the convergent movement of the target will be destroyed, and the energy gain will be reduced.

Second, the impacts of the phase difference on the maximum normalized thickness between the upper interface and the lower interface are studied using Eq. (5). This thickness can be represented by the normalized distance between the bubble of the upper interface and the spike of the lower interface along the acceleration direction. The reference quantity is the wavenumber. Figures 4(a)–4(c) present the temporal

evolutions of several phase differences under the conditions with several initial wavelengths ($kd = 0.2,\ 0.4$ and 0.8). The initial perturbation amplitudes on the two interfaces are 0.01λ. It is shown that the less the phase difference is, the less the maximum thickness will be. This implies that the temporal evolution of the RTI on the thin shell target is more serious when the phase difference is large. For the situation of anti-phase, the evolution of the RTI on the shell is fastest. In terms of the effects of the normalized thickness kd, the evolution of the RTI will be enhanced when kd is small.

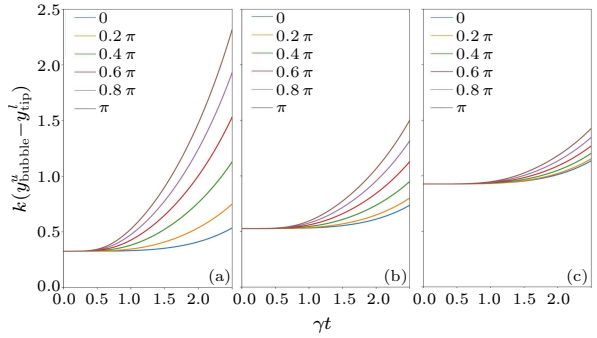

Fig. 4. Evolutions of maximum interface thickness under the conditions of several phase differences: (a) $kd = 0.2$, (b) $kd = 0.4$, (c) $kd = 0.8$.

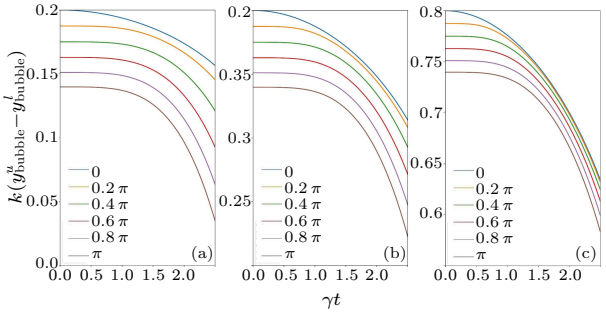

Fig. 5. Evolutions of minimum interface thickness under the conditions of several phase differences: (a) $kd = 0.2$, (b) $kd = 0.4$, (c) $kd = 0.8$.

Lastly, the impacts of the phase difference on the minimum normalized thickness between the upper interface and the lower interface are studied. It is located at the position of the bubble. Figure 5 presents their temporal evolutions. The initial wavelengths and the initial perturbation amplitudes are the same as those in Fig. 4. It is shown that the larger the phase difference is, the more quickly the target will change to be thick. This rule is right under the different initial normalized thicknesses. This means that the thin target is easier to tend to break when the phase difference is large.

In conclusion, a linear analytical RTI model including the phase effects is presented. The accuracy of the model is tested by the Euler numerical simulation. It is shown that: (1) the phase difference does not change the basic structure of the RTI that only one spike and one bubble are in a period. However, the spike and the bubble are distorted, which has an unexpected influence on the convergent movement of the target. (2) The distance between the spike and bubble along the vertical direction of acceleration differs by π. (3) When the phase difference is large, the temporal evolution of the long-wavelength RTI on a thin shell is more serious, and the thin target is easier to break.

References

[1] Rayleigh L 1883 *Proc. R. Soc. London Ser. A* **14** 170
[2] Taylor G 1950 *Proc. R. Soc. London A* **201** 192
[3] Wang L F et al 2017 *Sci. Chin.-Phys. Mech. Astron.* **60** 055201
[4] Lindl J D et al 2004 *Phys. Plasmas* **11** 339
[5] Atzeni S et al 2004 *The Physics of Inertial Fusion: Beam Plasma Interaction, Hydrodynamics, Hot Dense Matter* (Oxford: OUP Oxford)
[6] Mikaelian K O 1983 *Phys. Rev. A* **28** 1637
[7] Mikaelian K O 2005 *Phys. Fluids* **17** 094105
[8] Wang L F et al 2014 *Phys. Plasmas* **21** 122710
[9] Guo H Y et al 2017 *Chin. Phys. Lett.* **34** 075201
[10] Waddell J T et al 2001 *Phys. Fluids* **13** 1263
[11] Wilkinson J P and Jacobs J W 2007 *Phys. Fluids* **19** 124102
[12] Ye W H et al 2002 *Phys. Rev. E* **65** 057401